Adaptive Open-pit Mining Planning under Geological Uncertainty

Abstract

This research project developed an adaptive stochastic optimisation approach for multi-period production scheduling in open-pit mines under geological uncertainty, and compared it to an existing two-stage optimisation method. This new rolling-horizon optimisation approach updates the geological model each time period as new information becomes available. Numerical tests carried out earlier on open-pits of different sizes showed that, on average, the rolling-horizon adaptive policy gave better results than the non-adaptive two-stage approach. The metric used was the percentage gap between the results for each policy and those that would be obtained if the true block grades were perfectly known.

This paper extends this earlier work in two ways: firstly, by introducing a second metric — the dollar-value difference between the NPV generated with perfect knowledge of the orebody and those given by the other two optimisation methods. The rolling-horizon approach is still better on average than the two-stage approach, but not for all of the geostatistical simulations used to model the geological uncertainty. The second innovation in this paper is to analyse when the new rolling-horizon approach outperforms the non-adaptive one. This depends on the drill-hole spacing. For widely spaced grids, the rolling-horizon approach statistically outperforms the two-stage approach at the 95% confidence level. For very close spacings, both approaches converge toward the results for perfect knowledge.

Keywords: Stochastic optimisation, adaptive algorithms, learning, geostatistical simulations.

1 Introduction

This paper continues a research project initiated by the authors of Lagos et al. (2020) which developed an adaptive stochastic optimisation approach for multi-period production scheduling in open-pit mines under geological uncertainty, and compared it to the non-adaptive two-stage optimisation method developed by Moreno et al. (2017). The new approach is a rolling-horizon optimisation that updates the orebody block model each time period as new information becomes available as mining advances. Geological uncertainty on the grades in the deposit was modelled, as is usual, by generating geostatistical simulations (i.e. equally likely realisations of the deposit given the available data). As we used a very efficient updating algorithm described in Section 2.5, we can afford to use a large number of simulations (100, in our case) and still have a reasonable computation time.

In earlier work Lagos et al. (2020) showed that this rolling-horizon adaptive policy gave better results, on average, than the non-adaptive two-stage approach but this does not mean that it was always better. The aim of this paper is to study this in more detail for different sized pits and for different drill-hole spacings and to introduce a second metric for comparing the results — one that is more relevant in the mining industry, namely, the dollar-value difference between the net present value (NPV) generated with perfect knowledge of the orebody and that given by the other two optimisation methods. The metric used earlier in Lagos et al. (2020) was the percentage gap between the results for each policy and those that would be obtained if the true grades had been perfectly known as this is the standard metric used in operations research. Using the new dollar-value metric, we show that the rolling-horizon approach is still better on average than the two-stage approach, especially for wide drill-hole spacings, but it is not better for all of the simulated orebody block models used to model geological uncertainty. The percentage of cases where the rolling-horizon optimisation outperforms the two-stage optimisation depends on the drill-hole spacing. For widely spaced grids, the rolling-horizon approach is better more often. For closely spaced drill-holes (20m $\times$ 20m or 40m $\times$ 40m), both approaches converge toward the results for perfect knowledge.

The paper is structured as follows. In Section 2 we review the literature on mine planning optimisation, focusing on two approaches that are similar to ours: the work by Moreno et al. (2017), and the one by Dimitrakopoulos and Jewbali (2013) and Jewbali and Dimitrakopoulos (2018). We also review how geostatistical simulations are being used to model geological uncertainty. Section 3 presents the two methods compared here (Moreno's two-stage optimisation and our rolling-horizon one). In Section 4 the five case studies considered are described. The numerical results are presented in Section 5 which is divided into three subsections. In Section 5.1, after showing that the gaps for both policies converge to zero as the grid mesh shrinks, we used a one-sided paired t-test show that the rolling-horizon policy is statistically better (at the 95% confidence level) than the two-stage policy for the wider spaced grids, except for the 20 $\times$ 20m grid. In Section 5.2, we use the concept of integral range to explain how variable the NPVs are for the perfect knowledge case for widely

spaced grids. In Section 5.3, the NPV of the rolling-horizon policy divided by the NPV of the corresponding perfect knowledge case is compared to that of non-adaptive policy. Section 6 gives our conclusions and perspectives for future work.

2 Literature review

The aim of stochastic mine planning is to optimally schedule mining activities over time while still complying with precedence and resource usage constraints (see Hustrulid et al. (2013) and Stone et al. (2018) for details on the constraints that impact open-pit mines) and while taking account of uncertainty, sometimes on the commodity price but usually on the orebody block model.

2.1 Modelling uncertainty in mining projects

As the annual cashflow of a mine equals the revenue (i.e. the quantity of the product sold times the sales price) minus the fixed plus variable costs, there are two main types of uncertainty: uncertainty on the costs and the commodity price, and uncertainty on the ore grades, material types, geometallurgical properties, etc. Despite the importance of costs and commodity prices, few papers have modelled financial uncertainty. One exception is Richmond (2018) who used a two-factor Pilipovic model for copper prices and Black and Scholes model for extraction and mining costs. Others include Henry et al. (2005), Meagher et al. (2010), Asad and Dimitrakopoulos (2013), Kizilkale and Dimitrakopoulos (2014), Chatterjee et al. (2016), Mokhtarian Asl and Sattarvand (2018) and Rimélé et al. (2020).

Far more effort has been focused on modelling uncertainty on ore grades, typically by using geostatistical simulations of the deposit given the information available. These numerical models are possible realisations of the deposit (see Section 2.5 for details). Since the 1990s the effect of different drilling patterns and mine plans has been tested on them (Ravenscroft, 1992; Dowd, 1994; Khosrowshahi et al., 2018; Godoy, 2018; Tahernejad et al., 2018; Vallejo and Dimitrakopoulos, 2019; Maleki et al., 2020). Tavchandjian et al. (2018) used conditional simulations to choose the most appropriate mining method and mining equipment and Dowd and Dare-Bryan (2018) used them to study blast design and to model ore dilution.

In this paper, we compare two policies for multi-period production scheduling under geological uncertainty but do not consider financial uncertainty. The main reason is that, except for oligopolistic markets, the latter uncertainty is exogenous to the mining project and equally affects the two policies under consideration. What makes the difference between both policies is the way they handle geological uncertainty. Unlike financial uncertainty, geological uncertainty is endogenous to the production scheduling problem: it affects the decisions taken on which blocks to extract in a given time period and these decisions affect how the orebody is mined and make it possible to reduce the uncertainty locally as the extracted blocks provide knowledge of the true ore grades.

2.2 Review papers

Two excellent reviews of optimisation applied to mining planning were published in 2008 and 2010, namely Osanloo et al. (2008) and Newman et al. (2010). Both start out by presenting the early deterministic approaches (Lerchs and Grossmann, 1965; Gershon, 1987) and go up to the early uncertainty-based approaches. Whereas Osanloo et al. consider only open-pit mines, Newman et al. also discuss underground mining. Readers interested in developments up to 2010 can consult these two papers. We shall concentrate our attention on more recent publications. In addition to these two review papers, the book edited by Dimitrakopoulos (2018) presents an overview of *state-of-the-art* practices in the mining industry.

2.2.1 Two 2-stage production scheduling models with geological uncertainty

As our research follows on from work by Moreno et al. (2017), and by Dimitrakopoulos and Jewbali (2013) and Jewbali and Dimitrakopoulos (2018), we describe them in detail. All three developed two-stage production scheduling models for open-pit mine planning under geological uncertainty and used a set of conditional geostatistical simulations to model that uncertainty. Both tested their approaches on a real deposit: Moreno et al., on a copper deposit and Jewbali and Dimitrakopoulos, on a producing gold mine. However there are some important differences between the two. Firstly whereas Moreno et al. maximised the expected net present value, the objective function in the other work also contained penalty terms for producing more or less than in the production plan. Moreno et al. addressed the proposed integer programming model by reformulating it as a large-scale precedence constrained knapsack problem that can be solved (nearly optimally) using a modified version of the Bienstock-Zuckerberg decomposition (Bienstock and Zuckerberg, 2010). The procedure in Moreno et al. can be summarised as follows:

- Stage 1: The scheduling decision is made; this assigns the time when each cluster (bench-phase or similar) will be extracted.
- Stage 2: When the true ore grade is revealed (from blast-holes or by grade control drilling), the model decides how to treat each individual block in that cluster (i.e. whether to send it to the processing plant or the waste dump).

In contrast to Moreno et al. who assumed that the ore block grades were perfectly known once the blast-hole data were available, Jewbali and Dimitrakopoulos (2018) considered that the grade control drilling merely gave much more accurate predictions of the grades of blocks to be extracted. So they needed to update the conditional simulations based on sparse exploration drilling, to incorporate the new grade control data. This was the key innovative feature of their work. Their optimisation process is divided into four stages:

- Stage 1: Generate a set of high density future grade control data for incorporation into the production scheduling process by using sequential Gaussian co-simulation and a joint spatial

correlation model between exploration data and grade control data available in previously mined out parts of a deposit.

- Stage 2: Update the pre-existing simulated orebody models based on the simulated future grade control information, by using conditional simulation by successive residuals (Jewbali and Dimitrakopoulos, 2011).
- Stage 3: A stochastic programming mine scheduling formulation handles multiple simulated orebody models from Stage 2. The objective function maximises NPV while minimising deviations from production targets.
- Stage 4: The risk in the produced schedules generated is quantified and the schedules are compared.

2.3 Recent papers

Two broad streams can be distinguished in recent papers: those by specialists in operations research which focus on optimal solutions for large sized mines, and those which focus on modelling the mining system in more detail (multiple pits, complex processing plants, blending and stockpiles, etc). The latter usually have recourse to meta-heuristics to solve the systems (Lamghari, 2017). One exception is Rezakhah et al. (2020): after having found that the linear programming relaxation of their objective function is unimodal, they adapted an existing linear program to an operational gold-copper open pit where a stockpile is used to blend materials based on multi-block characteristics.

2.3.1 Meta-heuristics

Most mine planning optimisation papers, including this paper, assume that once material is excavated it is sent either to the waste dump or to the processing plant. In practice stockpiles are often included for blending or to store excess material or low-grade material that will be processed later. The fact that newly arrived material is mixed with the rest of the stockpile complicates the optimisation because it leads to quadratic constraints. Bley et al. (2012) studied several solvers for mixed integer quadratically constrained programs and tested them on two case studies, one with 8513 blocks aggregated into 85 panels and the other with 96,821 blocks aggregated into 125 panels. Paithankar et al. (2020) used three heuristics (a genetic algorithm, a maximum flow algorithm and a cut-off grade algorithm) to solve a complex non-linear problem with stockpiling and grade uncertainty, applied to copper and gold operations.

In export supply chains consisting of mining, ore processing, transportation to the port, stockyard management and vessel loading, the different subsystems are usually studied in isolation with little consideration for their interactions with upstream and downstream subsystems (Bodon et al., 2018). Balzary and Mohais (2018) used simulation models supported by metaheuristic optimisation techniques to develop decision support systems for supply chains for bulk materials such as coal and iron ore.

Goodfellow and Dimitrakopoulos (2016) modelled a copper-gold deposit with six possible destinations for material: the sulphide mill, the sulphide heap leach, the sulphide waste dump, the transition heap leach, the oxide heap leach and the oxide waste dump. They considered uncertainty on grades of both the primary metal and the secondary elements, and on the material types (oxides, sulphides and transition material). They proposed a two-stage stochastic optimisation that involves three combinations of metaheuristics including simulated annealing, particle swarm optimisation and differential evolution.

As sustainable development is becoming an increasingly important topic for the mining industry, companies are concerned to reduce the environmental impact of waste dumps and stockpiles. When the deposit consists of low dip layers with a long strike, waste can be dumped in the pit (Zuckerberg et al., 2007). Rimélé et al. (2018) and Spleit (2018) have developed a stochastic integer program for these types of deposits and have tested it on iron-ore deposits.

2.3.2 Near-optimal solutions for larger pits

Solving the mathematical programming model for the strategic open-pit mine planning problem originally proposed by Johnson (1968), has been dauntingly difficult for real mines because their block models contain millions of blocks and production continues over decades. Block aggregation techniques, grouping blocks into larger mining units (Tabesh and Askari-Nasab, 2011; Jélvez et al., 2016; Mai et al., 2019), or decomposition approaches based on sliding time-windows and block preselection (Jélvez et al., 2019; Maleki et al., 2020), can be used to reduce the size of the optimisation problem. Boland et al. (2008) tackled the difficult case of stochastic programming with endogenous uncertainty (Goel and Grossmann, 2006). They considered uncertainty in the block grades and used *wait and see* decision schemes, where some of the decisions are taken only after the actual grades are revealed.

Advances in stochastic programming and robust optimisation over the last two decades (Shapiro et al., 2009; Ben-Tal et al., 2009) have also allowed the development of approaches with good theoretical properties. In particular, Lagos et al. (2011) compared the risk-hedging performance of three approaches for optimisation under uncertainty: Value-at-Risk, Conditional Value-at-Risk and a proposed robust optimisation approach, and tested them on a vein-type deposit. These developments have made it possible to get closer to the optimal solution for real deposits. Canessa et al. (2020) considered a risk-averse ultimate pit problem under geological uncertainty and derived conditions for generating a set of nested pits by varying the risk level instead of using revenue factors. They developed a two-stage stochastic programming formulation of the problem and an efficient approximation scheme to solve it. The approach was tested on a section of the Andina mine, in Chile.

Goycoolea et al. (2015) proposed an MIP model for scheduling the blocks in each of a set of predefined push-backs using the Bienstock-Zuckerberg algorithm and tested it on six different cases with up to 4 million blocks that produced for up to 60 time periods. The data for two of these studies are freely available to the public (Espinoza et al., 2013). For more information on

the Bienstock-Zuckerberg algorithm, see Bienstock and Zuckerberg (2009, 2010) and Muñoz et al. (2018).

2.4 Updating

As far as adaptive optimisation or optimisation with learning is concerned, Powell and Ryzhov (2012) is a a fairly comprehensive reference extending mostly from Bayesian approaches for the problem of *ranking and selection*. More recently, Frazier (2018) deepened in the direction of Bayesian optimisation with Gaussian process regression.

From the late 1980s on, Bayesian analysis has been combined with geostatistics (Omre, 1987; Christakos, 1990; Omre and Tjelmeland, 1997; Benndorf, 2015), but it was used mostly to model uncertainty on the parameters of the spatial covariance or to obtain improved spatial predictions. More recently, McKinley et al. (2014) used geostatistical Bayesian updating to integrate airborne radiometrics and soil geochemistry to improve maps for mineral exploration. Willigers et al. (2014) combined geostatistics and Bayesian updating to continually optimise drilling strategies in shale-gas plays.

As will be seen in the next section, different models and algorithms exist for generating geostatistical simulations and the algorithms based on multivariate Gaussian models are more suitable for updating. For example, in the oil industry, they are used for *history matching*, that is, updating reservoir models as production figures become known, see Oliver et al. (2008) and Oliver and Chen (2011). Coming back to mining, Goria (2004), working in a real option framework, used geostatistical simulations to determine the value of additional drilling for a gold deposit.

2.5 Geostatistical simulations

There are many different methods for constructing realisations of ore grades, such as sequential approaches (Gómez-Hernández and Journel, 1993; Soares, 2001; Dimitrakopoulos and Luo, 2004), spectral approaches (Lantuéjoul, 2002; Chilès and Delfiner, 2012; Emery et al., 2016) or high-order simulations (Mustapha and Dimitrakopoulos, 2010; de Carvalho et al., 2019), but most are not suitable for updating orebody block models as new information becomes available. Our updating method uses the good properties of the multivariate Gaussian distribution and requires holding the original Gaussian unconditional simulation and conditioning it with the new data as well as the old. The main steps are:

- The raw data (ore grades) are converted to their Gaussian equivalents.
- The experimental spatial covariance function (or equivalently the variogram) of the Gaussian equivalents is computed and a theoretical covariance or variogram model is fitted.
- The required number of unconditional realisations are generated.
- These are "conditioned" to the available data (drill-hole data or block grades), by means of a post-processing step based on kriging.

- Finally these are back-transformed to grades in the raw scale.

For more information on geostatistical simulations readers can consult Goovaerts (1997), Lantuéjoul (2002) or Chilès and Delfiner (2012). Some code for generating these unconditional and conditional realisations is given by Emery and Lantuéjoul (2006).

Our rolling-horizon policy requires being able to generate many orebody realisations (in our case 100) in each time period, conditioned not only to the drill-hole data, but also to the observed grades from the blocks extracted in previous periods. Instead of computing these realisations from scratch in each time period, it is much more efficient to use the same set of underlying unconditional realisations and to update them to the newly available data. This is possible because each conditional realisation is built on the basis of an unconditional realisation that, by definition, does not need to be updated when new data becomes available. In other words, the same set of 100 unconditional realisations is used for all the time periods and one just needs to recalculate the kriging weights in order to convert the unconditional realisations into conditional realisations (in a post-processing step). Further computational simplifications are possible if one takes account of the relationships between the kriging weights calculated by using a set of data and those calculated by using a subset of these data (Chevalier et al., 2015).

3 Optimisation models

Now we present the basic mixed integer programming model for the two policies considered in this work, the non-adaptive two-stage (2S) and the adaptive rolling-horizon (RH) policies. We proceed as follows: in Table 1 we define the elementary sets, the basic parameters, and the variables considered in the mathematical model, then we present the mixed integer two-stage stochastic model, and finally we explain in detail the aforementioned policies.

The model is the following:

$$\max \quad \sum_{t\in T} \frac{1}{|S|} \left[\sum_{b\in B,\, s\in S} v^s_{b,t}\, y^s_{b,t} - \sum_{i\in\mathcal{C}} w_{i,t}\, \theta_{i,t} \right]$$

$$\text{s.t.} \quad \sum_{t\in T} \theta_{i,t} \le 1 \qquad \forall\, i \le m \tag{1a}$$

$$\theta_{i,t} \le \sum_{s\le t} \theta_{j,s} \qquad \forall\, (i,j)\in P, \quad t\in T \tag{1b}$$

$$\sum_{i\le m} \theta_{i,t}\, k^{ex}_i \le K^{ex} \qquad \forall\, t\in T \tag{1c}$$

$$y^s_{b,t} \le \theta_{i,t} \qquad \forall\, i\in\mathcal{C}, \quad b\in B_i, \quad t\in T, \quad s\in S \tag{1d}$$

$$\sum_{b\le n} y^s_{b,t}\, k^{pr}_b \le K^{pr} \qquad \forall\, t\in T, \quad s\in S \tag{1e}$$

$$\theta_{i,t} \in \{0,1\} \qquad \forall\, i\in\mathcal{C}, \quad t\in T \tag{1f}$$

$$0 \le y^s_{b,t} \le 1 \qquad \forall\, b\in B, \quad t\in T, \quad s\in S. \tag{1g}$$

B	Index set of blocks, each $b \in B$ represents a production unit in the mine
$\mathcal{C}$	Set of clusters of blocks, each $i \in \mathcal{C}$ contains several blocks
$B_i \subseteq B$	Set of blocks contained in cluster $i \in \mathcal{C}$
T	Set of time periods considered for the exploitation and processing of the material from the mine
$P \subseteq \mathcal{C} \times \mathcal{C}$	Precedence set between clusters of the mine, each element $(i, j) \in P$ defines a precedence. Cluster i must be exploited not later than cluster j
S	Finite set of scenarios of the ore content of blocks. Each scenario determines a possible realisation of the ore content of all blocks $b \in B$
K^{ex}	Maximum extraction capacity for each time period
k_i^{ex}	Extraction rate for extracting cluster $i \in \mathcal{C}$
K^{pr}	Maximum processing capacity for each time period
k_b^{pr}	Rate for processing the ore content of block $b \in B$
$w_{i,t}$	Total cost incurred by extracting cluster $i \in \mathcal{C}$ at time period $t \in T$, discounted by the difference of number of periods with respect to period 1
$v_{b,t}^s$	Profit obtained by the processing a unit of block $b \in B$ at time period $t \in T$, under scenario $s \in S$, brought to present value with respect to period 1
$\theta_{i,t} \in \{0, 1\}$	Binary variable that is equal to 1 if and only if all blocks in B_i, $i \in \mathcal{C}$ are excavated in time period $t \in T$
$y_{b,t}^s \in [0, 1]$	Continuous variable that denotes the portion of block b that is processed in period $t \in T$, under scenario $s \in S$

Table 1: Sets, parameters, and variables considered in the mathematical model, partitioned by double lines, respectively.

The two-stage mixed integer stochastic program of Model (1) maximises the net present value given by the extraction and processing decisions. Constraint (1a) ensures that each cluster is extracted at most once; Equation (1b) requires that the optimal solution must respect the prescribed precedence given in set P, (1c) limits the extraction capacity of each time period; while (1d) requires the solution to allow to process blocks that belong to a cluster extracted in the same time period in which the block is processed, Equation (1e) limits the processing capacity for each time period and Constraints (1f) and (1g) impose the support for the variables in the Model.

Both policies presented in this section follow a similar framework. First, a set of scenarios of block grades is generated using the available data from drill holes samples. Then, in each time period the policy determines the extraction decisions and subsequently executes the processing decisions by optimally solving a very simple continuous knapsack problem. The frame can be outlined as follows:

- Generate the next geostatistical simulation of block grades conditioned on drill-hole data, out of a set of S simulations.
- For $t \in T$:
  1. Set extraction decisions, $\theta_{i,t}$ for period t according to the solution of the model, where $\theta_{i,t} = 1$ if and only if cluster $i \in \mathcal{C}$ is extracted.

2. Set processing decisions for period t according to the solution to

$$\max \left\{ \sum_{i:\theta_{i,t}=1} \sum_{b \in B_i} v_{b,t}\, y_b : \sum_{i:\theta_{i,t}=1} \sum_{b \in B_i} y_b\, k_b^{pr} \leq K^{pr},\, 0 \leq y_b \leq 1 \;\forall\; b \leq n \right\}.$$

Now we present the first policy considered in this study, the 2S policy. It follows the extraction decisions given by the solution of Model (1), that is, for any time period $t \in T$, we extract cluster $i \in \mathcal{C}$ if and only if $\theta_{i,t}$ is equal to one. The second policy, RH, updates the set of S geostatistical simulations of block grades in each time period before the extraction is executed (except in period 1). More specifically, in the first time period the extraction executed and the set of scenarios considered are the same as in the 2S policy, then, in subsequent periods, the set of scenarios considered is conditioned on observed grades from blocks already extracted and on drill-hole data, then it proceeds by reformulating and solving Model (1) with the extraction decisions for periods $s < t$ fixed.

4 Set-up for computational experiments

4.1 Layout of the drill holes relative to the blocks.

In our model, blocks are 10m $\times$ 10m $\times$ 10m and drill hole samples are 10m long. The average grade of each sample or block is situated at its center. Different drill-hole grids were considered: 20m $\times$ 20m, 40m $\times$ 40m, and so on. If the grid spacing is halved, the number of drill holes is quadrupled.

Figure 1 illustrates the layout for the top bench for two of the cases considered (Nos. 7 and 10), which is 320m $\times$ 320m. It contains 1024 (i.e., 32 $\times$ 32) blocks with black dots indicating their centers. Drill holes located at the corners of the blocks are shown in red or blue depending on the spacing. The blue circles represent drill holes on a 40m $\times$ 40m grid, while the red ones are on a 20m $\times$ 20m grid and some red ones are covered up by blue ones.

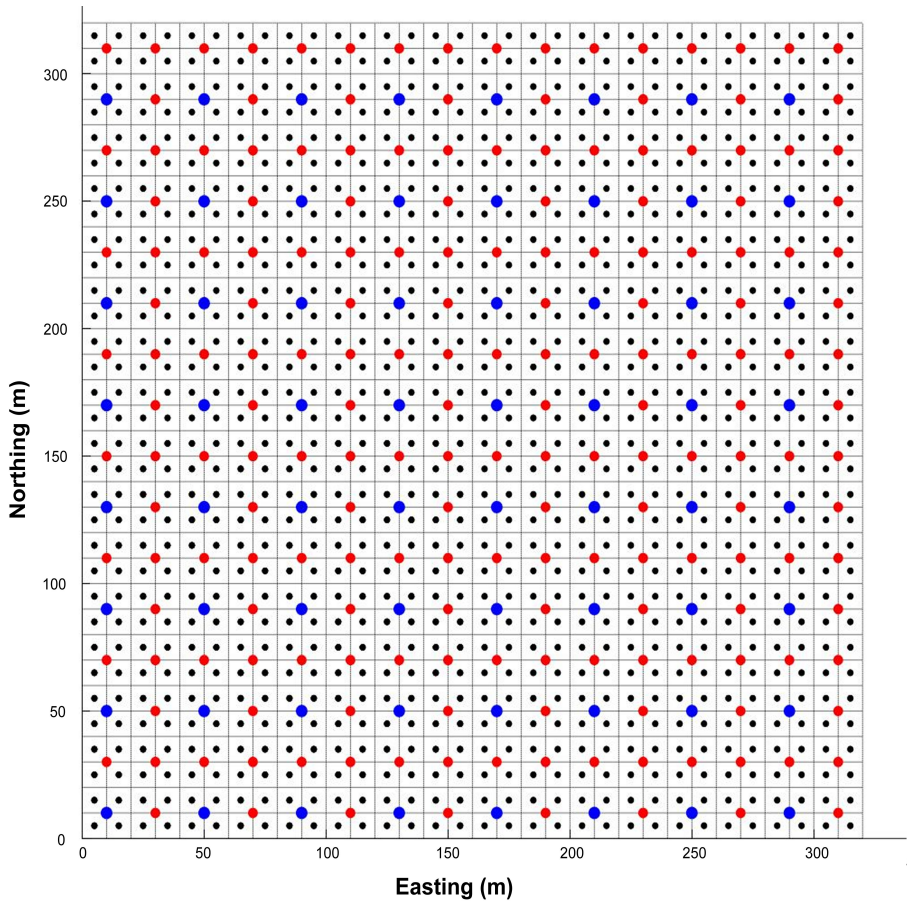

Figure 1: **Layout of Drill holes relative to Blocks:** a zone 320m $\times$ 320m containing 1024 (i.e., 32×32) blocks each 10m by 10m with black dots indicating their centers. Drill holes shown in red or blue depending on the spacing are located at the corners of the blocks. The blue circles are on a 40m by 40m grid while the red ones are on a 20m by 20m grid and some are covered up by blue ones on the wider spaced grid.

Presenting the set-up more formally. We tested the performance of two policies, Moreno et al.'s two-stage approach (2S) and the new rolling-horizon approach (RH), in addition to perfect knowledge (PK), in which the true ore grades are known at the outset and so there is no uncertainty. The PK policy provides an unattainable upper bound on performance.

Our aim is to study the impact of the number of drill holes and the number of blocks on the extraction policy π, for each $\pi \in \{\text{PK, 2S, RH}\}$. To do this, we parameterise the mine by constants m and ℓ with $m \geq 2$. The set X_{DH} defines the locations of samples in drill holes as follows:

$$X_{DH} = \left\{(x_1, x_2, x_3) = (20i, 5 + 20(j-1), 5 + 10(k-1)) \in \mathbb{Z}^3 \,:\, i, j \in \{1, \ldots 2^{m-1}\},\, k \in \{1, \ldots, \ell\}\right\}. \tag{2}$$

Accordingly, there are $2^{m-1} \times 2^{m-1} = 2^{2(m-1)}$ drill holes in the horizontal (x_1, x_2) plane, each containing ℓ samples aligned vertically. In some of the experiments, we took a smaller subset of 2^{2r} points in X_{DH} $(r = 0, \ldots, m-1)$ in such a way that points were equally spaced on the horizontal

plane. Similarly, the set of blocks $\tilde{X}_{Block}$, is defined as follows:

$$\tilde{X}_{Block} = \left\{(x_1, x_2, x_3) = 5 + 10(i-1, j-1, k-1)) \in \mathbb{Z}^3 \,:\, i, j \in \{1, \ldots 2^m\},\, k \in \{1, \ldots, \ell\}\right. . \quad (3)$$

The total number of blocks in $\tilde{X}_{Block}$ is $2^m \times 2^m \times \ell = 2^{2m}\ell$. Because of the slope stability constraint, not all blocks in $\tilde{X}_{Block}$ are feasible for extraction. Let $X_{Block} \subset \tilde{X}_{Block}$ be the set of blocks that can be extracted.

Next we define the precedence constraints. In open pits, a block cannot be extracted until the blocks above have been removed. For that, we index blocks in X_{Block} with the set $B := \{1, \ldots, |X_{Block}|\}$ from the top to down, so that if block b_1 is closer to the surface than block b_2, then $b_1 < b_2$. We first define precedence constraints at the block level as follows:

$$P_{Block} = \left\{(b_1, b_2) \,:\, |x_1^{b_1} - x_1^{b_2}| \leq 10,\, |x_2^{b_1} - x_2^{b_2}| \leq 10,\, x_3^{b_2} = x_3^{b_1} + 10, 1 \leq b_1 < b_2 \leq |B|\right\}. \quad (4)$$

With these constraints, we defined the set P by using a bench-phase design (see, e.g., Moreno et al. (2017)) considering precedence constraints for adjacent clusters in the North-South and West-East directions, and also in the top-down direction.

4.2 Values of key parameters

We set the extraction capacity as

$$K^{ex} = \frac{1}{|T| + 1} \sum_{b \in B} \text{weight}_b, \quad (5)$$

where weight_b denotes the weight of block b. The processing capacity K^{pr} is half of that amount. The numerical values of the parameters taken from Moreno et al. (2017) are listed in Table 2.

Commodity (copper) price	2.1 USD/lb	Discount factor	10%
Mining cost	2.5 USD/ton	Processing cost	10 USD/ton

Table 2: **Key costs and technical parameters used to run numerical tests:** These values come from Moreno et al. (2017)

.

4.3 Geostatistical simulations

For each study, 100 geostatistical simulations (scenarios) were constructed using the turning bands method (Matheron, 1973; Emery and Lantuéjoul, 2006). The spatial covariance of the Gaussian equivalents of ore grades consisted of the sum of an isotropic spherical structure with a correlation range of 100m and a sill of 0.45, an isotropic exponential structure with a practical range of 100m

(scale parameter 100/3) and a sill of 0.45 and nugget effect of 0.1.

$$C(h) = \begin{cases} 0.45(1 - \frac{3}{2}\frac{|h|}{100} + \frac{1}{2}\left(\frac{|h|}{100}\right)^3)\mathbb{1}\{|h| < 100\} & \text{(spherical)} \\ +0.45\exp\left(-3\frac{|h|}{100}\right) & \text{(exponential)} \\ +0.1\,\mathbb{1}\{h = 0\} & \text{(pure nugget),} \end{cases} \tag{6}$$

where $\mathbb{1}\{\cdot\}$ denotes the indicator function, h is the separation vector between data and $|h|$ is the norm of h. The low nugget effect (only 10% of the total sill) and the long range relative to the size of the deposit mean that the Gaussian equivalents of the ore grades show good continuity. The function used to back-transform the Gaussian values to grades was close to an exponential, i.e., the ore grades have a distribution close to lognormal. This covariance model and back-transformation were those used by Moreno et al. (2017) and are typical of copper deposits.

4.4 Cases considered

In this research project the performance of the policies was tested numerically using a HP ProLiant SL230s Gen8 computer with 20 cores available (2 × Intel Xeon E5-2660 10 cores each). With five of these machines, we were able to parallelise all 100 realisations (scenarios) for each instance.

Lagos et al. (2020) carried out numerical tests for 14 cases ranging from artificially small to realistically-sized mines with more than 100,000 blocks, and for a variety of drill-hole spacings. Here we re-visit five of the realistic-sized cases studied in that paper, namely Nos. 7, 10, 12, 13 and 14. Table 3 lists the number of blocks (each 10m by 10m by 10m) along the three axes, together with the total number of blocks considered. As we assumed that the walls were inclined at 45° to ensure the slope stability of the open pit (Eq. (4)), there are fewer blocks at lower levels.

Case	Along X	Along Y	Along Z	# Total Number of Blocks.	# Instances Solved to optimality.
7	320m	320m	60m	4444	100
10	320m	320m	80m	5168	98
12	640m	640m	140m	37,324	92
13	1280m	1280m	60m	90,844	99
14	1280m	1280m	80m	117,926	61

Table 3: **Parameters used to run numerical tests:** columns 2, 3 and 4 give the number of blocks along X, Y and Z, in the orebody. The fifth column gives the total number of blocks, taking account of the slope stability angle, 45°. The last column has the number of instances solved out of 100 within a 3 hour time limit.

Table 4 gives the number of blocks, the extraction capacity, the number of precedences, the number of clusters and hence the average number of blocks per cluster, for the five cases considered in this paper.

Case	Number of Blocks	Extraction Capacity	Number of precedences	Number of clusters	Av No Blocks per Cluster
7	4444	740.67	104	48	92.58
10	5168	861.33	144	64	80.75
12	37,324	6220.67	264	112	333.25
13	90,844	15,140.67	104	48	1892.58
14	117,296	19,549.33	144	64	1832.75

Table 4: **Key parameters used to run numerical tests:** the number of blocks, the extraction capacity, the number of precedences, the number of clusters and hence the average number of blocks per cluster, for the five cases considered in this paper.

4.5 Two criteria for measuring policy performance

In the operations research community, the standard measure of the performance of an optimisation method is the gap between the actual performance and the optimum, expressed as a percentage. This is possible either when the optimum is known theoretically, or when working with synthetic cases where the "true" ore grades are known by construction. In our case, we computed this as $1 - RH/PK$ and $1 - 2S/PK$ where RH, 2S and PK refer to the results given by these methods. The averages were computed over the 100 out-sample simulations in each case.

However, in the mining industry, new methods are usually tested on real deposits by comparing the percentage improvement in the cumulative discounted cash flow or the NPV generated by the new approach compared to industry standards, e.g. Moreno et al. (2017), Menabde et al. (2018), and Maleki et al. (2020). In addition to computing the improvement in the NPV, Jewbali and Dimitrakopoulos (2018) also evaluated the increase in ore mined and the metal produced. In our case we computed the average NPV for the policies in million USD.

5 Results of the computational experiments

5.1 Average results over geostatistical scenarios

Tables 5 to 9 give the averages of the two criteria, the gap and the NPV, for the two policies and also the average NPV for perfect knowledge, PK, for the various drill-hole spacings, for the five cases considered. The number of drill holes acts as a proxy for the amount of knowledge policies have a priori. The results confirm that both policies converge to the perfect knowledge results as the drill-hole spacing decreases, i.e., as the amount of information increases. For both large and small mines, the 2S and RH policies lead to gaps of less than 5% of the upper bound given by the PK policy for the closest drill-hole spacings. Note the value for perfect knowledge PK does not change with the drill-hole spacing. As expected, the RH policy produces even smaller gaps than those obtained with 2S. Overall, both policies give very good results on average for large and small orebodies, even when there are very few drill holes, because the spatial covariance is well-structured

(low nugget effect and long correlation range). Having said that, in the next section we will see that there is considerable variability in the results from one simulation to another, especially for Cases 7 and 10.

Drill-hole Spacing	Number Drill holes	1-Gap 2S	1-Gap RH	NPV 2S	NPV RH	NPV PK
20m × 20m	256	0.995	0.995	868.15	868.08	872.19
40m × 40m	64	0.993	0.993	866.37	865.87	872.19
80m × 80m	16	0.982	0.986	856.97	859.84	872.19
160m × 160m	4	0.963	0.977	839.76	851.73	872.19

Table 5: **Mean values of the gap and the NPV for the rolling-horizon policy (RH) and the two-stage policy (2S) for Case No 7. The NPVs are in millions USD.**

Drill-hole Spacing	Number Drill holes	1-Gap 2S	1-Gap RH	NPV 2S	NPV RH	NPV PK
20m × 20m	256	0.997	0.997	898.35	898.50	901.03
40m × 40m	64	0.996	0.996	897.06	897.41	901.03
80m × 80m	16	0.985	0.991	887.06	892.85	901.03
160m × 160m	4	0.961	0.981	864.42	883.53	901.03

Table 6: **Mean values of the gap and the NPV for the rolling-horizon policy (RH) and the two-stage policy (2S) for Case No 10. The NPVs are in millions USD.**

Drill-hole Spacing	Number Drill holes	1-Gap 2S	1-Gap RH	NPV 2S	NPV RH	NPV PK
20m × 20m	1024	0.998	0.998	913.91	914.47	915.82
40m × 40m	256	0.997	0.997	913.36	913.86	915.82
80m × 80m	64	0.992	0.994	909.14	911.04	915.82
160m × 160m	16	0.979	0.985	896.96	902.65	915.82
320m × 320m	4	0.964	0.980	883.37	897.57	915.82

Table 7: **Mean values of the gap and the NPV for the rolling-horizon policy (RH) and the two-stage policy (2S) for Case No 12. The NPVs are in millions USD.**

Drill-hole Spacing	Number Drill holes	1-Gap 2S	1-Gap RH	NPV 2S	NPV RH	NPV PK
20m × 20m	4096	0.999	0.999	882.68	883.08	883.81
40m × 40m	1024	0.998	0.999	881.54	882.69	883.81
80m × 80m	256	0.997	0.997	881.20	881.51	883.81
160m × 160m	64	0.989	0.991	874.07	875.93	883.81
320m × 320m	16	0.980	0.986	865.54	871.66	883.81
640m × 640m	4	0.976	0.984	862.01	869.65	883.81

Table 8: **Mean values of the gap and the NPV for the rolling-horizon policy (RH) and the two-stage policy (2S) for Case No 13. The NPVs are in millions USD.**

Drill-hole Spacing	Number Drill holes	1-Gap 2S	1-Gap RH	NPV 2S	NPV RH	NPV PK
20m × 20m	4096	0.999	1.000	899.44	899.82	900.13
40m × 40m	1024	0.999	0.999	898.93	899.64	900.13
80m × 80m	256	0.996	0.997	896.54	897.54	900.13
160m × 160m	64	0.989	0.991	889.90	892.16	900.13
320m × 320m	16	0.981	0.987	882.98	888.13	900.13
640m × 640m	4	0.977	0.984	879.72	885.43	900.13

Table 9: **Mean values of the gap and the NPV for the rolling-horizon policy (RH) and the two-stage policy (2S) for Case No 14.The NPVs are in millions USD.**

Note that the computations were carried out in a do-loop: a new geostatistical scenario was generated then the two policies were evaluated. Consequently, as the values of the two-stage policy and the rolling-horizon policy were computed for the same scenarios, the values are paired. So it is possible to test the difference between their NPVs using a paired t-test. Secondly we are only interested in a one-sided test to determine whether or not the RH policy improves the 2S policy. Table 13 gives the results of the paired t-tests for the various drill-hole spacings. It shows that the NPV of the rolling-horizon policy is significantly higher, at the 95% confidence level, than that of the two-stage policy for the grids except for the 20m × 20m spacing and the 40mx40m spacing for case 7. These exceptions are not important from a practical point of view because with such closely spaced drill-holes, the NPVs of both policies are very close to that of perfect knowledge. However we have demonstrated that the new method is statistically better for widely spaced grids.

No Drillholes	4	16	64	256	1024	4096
Case 7 Mesh	160m×160m	80m×80m	40m×40m	20m×20m	-	-
Case 7 Mean	11.97	2.87	-0.05	-0.07	-	-
Case 7 StDev	21.75	11.93	6.54	3.40	-	-
Case 7 t-value	5.50**	2.41**	-0.77	-0.21	-	-
No Drillholes	4	16	64	256	1024	4096
Case 14 Mesh	640m×640m	320m×320m	160m×160m	80m×80m	40m×40m	20m×20m
Case 14 Mean	5.70	5.15	2.26	1.00	0.70	0.38
Case 14 StDev	14.51	10.31	7.80	3.98	1.79	1.93
Case 14 t-value	3.93**	4.99**	2.90**	2.51**	3.93**	1.95

Table 10: **Results of a one-sided paired t test of whether the rolling-horizon policy outperforms the two-stage policy as a function of the number of drill-holes and the mesh of the drill-hole grid. The asterisks indicate statistically significant t-values.**

5.2 Variability of perfect knowledge NPVs between geostatistical scenarios.

So far, the mean values of the two criteria were computed by averaging the results over the 100 realisations generated. This masks the variability amongst the realisations. In fact, there is considerable variability in the NPVs from one realisation to another, even for the NPV for perfect knowledge. Table 11 shows the basic statistics of the perfect knowledge NPVs for all five cases. The variability is especially marked for cases Nos. 7 and 10. This is due to a lack of ergodicity of the random field representing the ore grades in the geostatistical model, because the orebodies are small relative to the range of the variogram.

Case	Minimum	Maximum	Mean	Max/Min	Coeff Var
7	497	1610	872.19	3.24	0.256
10	520	1530	901.03	2.94	0.251
12	669	1450	915.82	2.17	0.155
13	761	1030	883.81	1.35	0.071
14	755	1070	900.13	1.42	0.089

Table 11: **Statistics for perfect knowledge for the five cases.** The minimum, maximum and mean are in millions of USD

The lack of ergodicity can be seen by computing the integral range (Lantuéjoul, 1991; Lantuéjoul, 2002). If $Z(V)$ is the average value of a spatial variable (ore grade) over region V, the integral range, IR, is defined as

$$IR = \lim_{[V]\to\infty} [V] \frac{VarZ(V)}{\sigma^2} \tag{7}$$

where $[V]$ is the volume of V and $\sigma^2 = C(0)$ i.e. the variance of the variable at a point support. This limit exists for all the usual covariance functions (Yaglom, 1987). Their integral ranges are

given in Table 12.

Covariance	1D	2D	3D
Spherical	$3/4$	$\pi/5$	$\pi/6$
Exponential	2	2π	8π

Table 12: **Integral Ranges.** For the the unit-range spherical model and the unit-scale parameter exponential model, in 1D, 2D and 3D spaces. Source: Lantuéjoul (2002, Table 2)

As the integral ranges of the unit-range spherical model and the unit-scale parameter exponential model are $\pi/6$ and 8π, respectively, see Table 12), the integral range in our case (Eq. (6)) is:

$$IR = 0.1 \times 0 + 0.45 \times 100^3 \times \frac{\pi}{6} + 0.45 \times \left(\frac{100}{3}\right)^3 \times 8\pi = 654,479. \tag{8}$$

The volume of the deposit in Case No 7 is $320 \times 320 \times 60 = 6,144,000$ m^3, that is, 9.39 times the integral range. Despite its apparent size, the volume only "allows for 9.39 independent repetitions", which is clearly not enough to get a spatial average with little fluctuations across the realisations. We advise readers to compute the integral range of their covariance/variogram and compare it to the volume of the deposit being considered in order to be aware of expected statistical fluctuations.

5.3 Comparing the NPV of the rolling-horizon policy with that of the two-stage policy.

Next we compare the NPV of two-stage policy with that of the rolling-horizon policy for increasing numbers of drill holes for the two extreme cases: No 7 and No 14. In order to filter out the variability between scenarios, the NPVs were divided by the NPV for the perfect knowledge (PK) case. This ratio was plotted as a function of the number of drill holes expressed as a power of 4 because the number of drill holes quadruples each time the drill-hole spacing was halved. For example, for case 7 (Figure 2) there were 4, 16, 64 and 256 drill holes, corresponding to grids with meshes 160m $\times$ 160m, 80m $\times$ 80m, 40m $\times$ 40m and 20m $\times$ 20m. The upper and lower panels are for the two-stage policy and the rolling-horizon policy, respectively. The solid line shows the average of the ratio. Similarly for Figure 3 for Case 14, except that 6 grid spacings were considered. Looking at these two figures, we see two things: firstly, the NPVs of both policies converge to that of perfect knowledge PK, which is hardly surprising given that the closest data are on a 20m $\times$ 20m grid. Secondly for the widely spaced grids, the NPVs for the rolling-horizon policy are higher on average and less dispersed than for the two-stage policy.

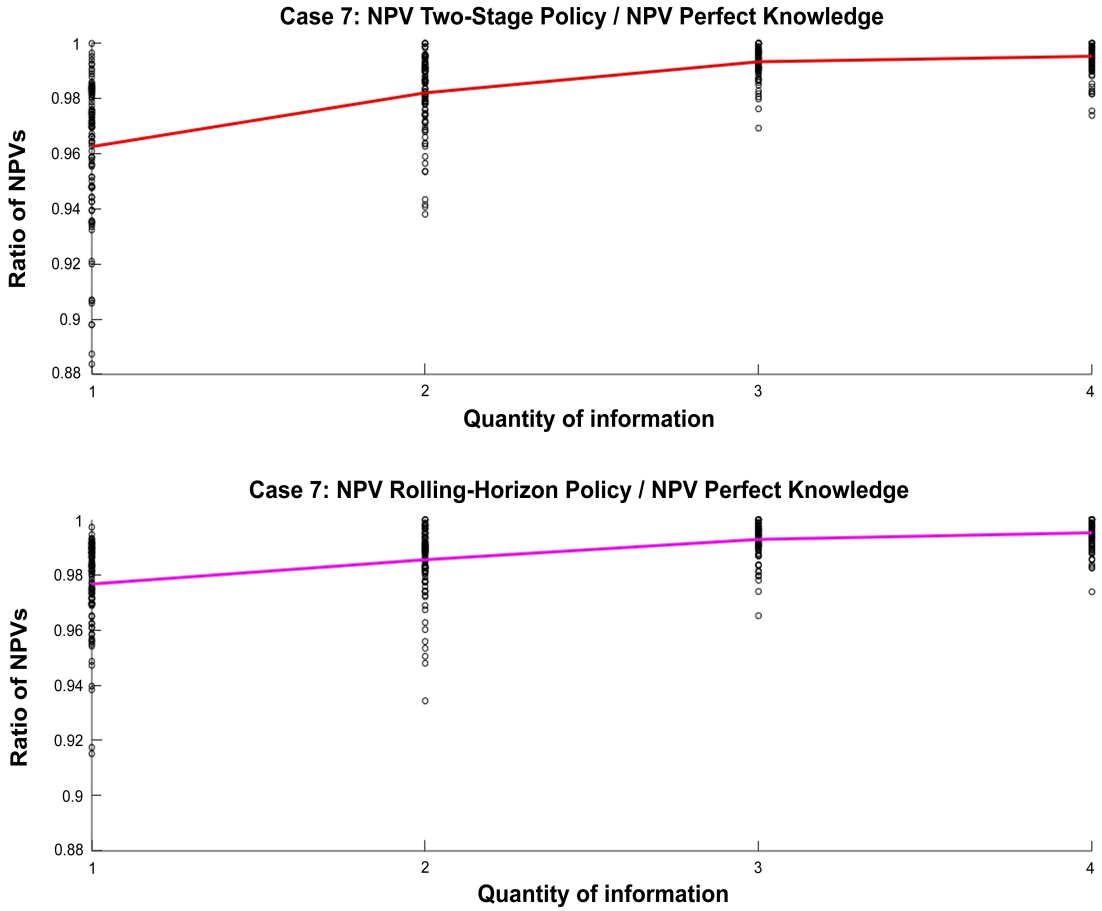

Figure 2: **Comparing the NPV of two-stage policy divided by NPV for PK (above) with the NPV of the rolling-horizon policy divided by NPV PK (below)** for increasing numbers of drill holes (from left to right, 4, 16, 64 and 256) for Case 7, with the solid line showing the average of the ratio.

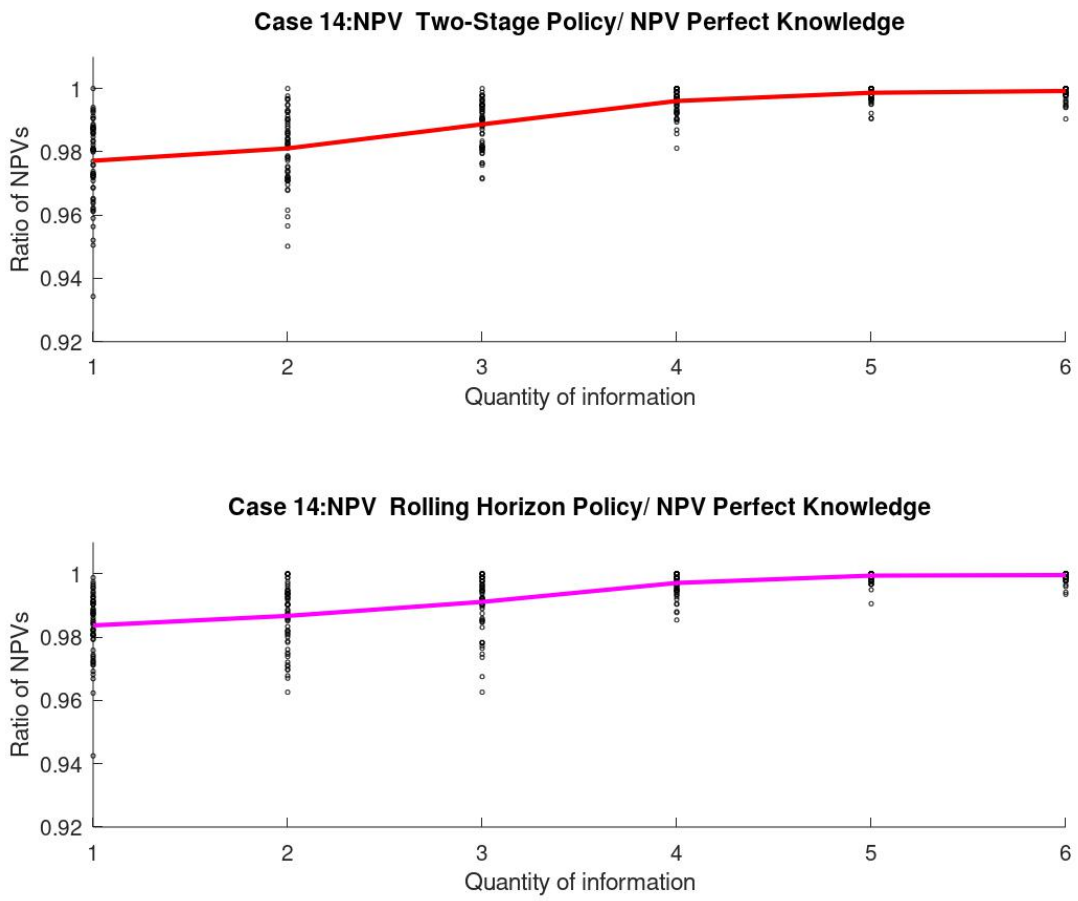

Figure 3: **Comparing the NPV of two-stage policy divided by NPV for PK (above) with the NPV of the rolling-horizon policy divided by NPV PK (below)** for increasing numbers of drill-holes (from left to right, 4, 16, 64, 256, 1024 and 4096) for Case 14, with the solid line showing the average of the ratio.

In Figure 4 the NPV of two-stage policy divided by NPV for PK was plotted against the NPV of the rolling-horizon policy divided by NPV for PK, for the widest spaced grid, for each of the 100 realisations for Case 7 (left) and Case 14 (right). The solid red line is at 45°; so for points above the line, the NPV for the rolling-horizon policy is higher than that for the two-stage policy. Note how much more dispersed the values are for Case 7 (the smaller zone). Table 13 gives percentage of geostatistical scenarios (simulations) for which the rolling-horizon policy outperforms the two-stage policy as a function of the number of drill-holes and the mesh of the drill-hole grid.

No Drillholes	4	16	64	256	1024	4096
Case 7	66%	55%	36%	24%	-	-
Case 7 Mesh	160m×160m	80m×80m	40m×40m	20m×20m	-	-
Case 14	55.7%	67.2%	55.7%	41.0%	36.1%	24.6%
Case 14 Mesh	640m×640m	320m×320m	160m×160m	80m×80m	40m×40m	20m×20m

Table 13: Percentage of geostatistical scenarios (simulations) for which the rolling-horizon policy outperforms the two-stage policy as a function of the number of drill-holes and the mesh of the drill-hole grid.

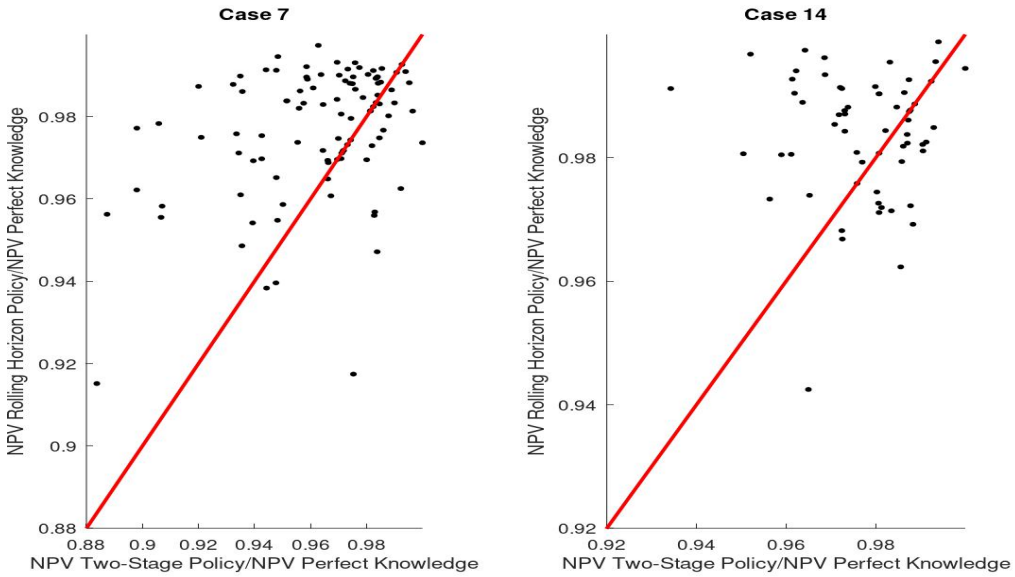

Figure 4: **Cross-plot the NPV of two-stage policy divided by NPV for PK with the NPV of the rolling-horizon policy divided by NPV for PK, for the widest spaced grid for Case 7 (left) and Case 14 (right)**

6 Conclusions and perspectives

This paper presents the second phase of a research project in which we developed an adaptive stochastic optimisation approach for multi-period production scheduling in open-pit mines under geological uncertainty, and compared it to an existing two-stage optimisation method and to the optimisation given perfect knowledge. This new approach is based on a rolling-horizon framework that updates the geological model each time period as new information becomes available. That is, we incorporate the fact that, as the deposit is mined, the true ore grades of mined-out material can be used to update the block model and re-optimise the production schedule of the remaining parts of the mine still to be exploited.

Numerical tests were carried out on synthetic open-pits of different sizes where, by construction, we knew the "true grades" and hence the perfect knowledge NPV. The metric used in the first phase

of this work (Lagos et al., 2020) was the percentage gap between the results for each policy and those that would be obtained if the true block grades were perfectly known. This showed that the rolling-horizon adaptive policy gave better results, on average, than the non-adaptive two-stage approach. However, while it is reassuring to know that the new approach is better on average, we need to know whether this happens for all geostatistical scenarios or just some of them, and in that case, which ones.

This paper extends earlier work in two ways, firstly by giving an in-depth statistical analysis of the results, and secondly, by introducing a second metric — the dollar-value difference between the NPV generated with perfect knowledge of the orebody and those given by the other two optimisation methods. The main contributions of this new analysis are:

- The average NPVs for the two-stage policy and the rolling-horizon policy converge to the average NPV for perfect knowledge as the grid mesh shrinks; likewise the average gaps for both policies converge to zero.
- Using a one-sided paired t-test we showed that the rolling-horizon policy is statistically better (at the 95% confidence level) than the two-stage policy for the wider spaced grids, but not for the 20m $\times$ 20m grid.
- This work highlighted the importance of the size of the deposit under study relative to the covariance structure. The values of the NPV for perfect knowledge turned out to be highly variable for the smallest two of the deposits considered. While their dimensions (320m $\times$ 320m $\times$ 60m and 320m $\times$ 320m $\times$ 80m) seem reasonable, the coefficients of variation for the NPVs were surprisingly high. This is due to ergodicity problems. We recommend computing the integral range before carrying out geostatistical simulations, to avoid surprises like this.
- Comparing the NPVs of the two policies showed that even though the rolling-horizon approach gives better results on average, this is not true for all geostatistical scenarios. The percentage of cases where the rolling-horizon optimisation outperforms the two-stage optimisation varies from about 25% to 65% depending on the drill-hole spacing. For very close spacings, both approaches converge toward the results for perfect knowledge. For widely spaced grids, the rolling-horizon approach is better more often.

6.1 Future Work

6.1.1 Moving beyond the assumption of a homogeneous rock mass

At the outset of this work, we made some simplifying assumptions about the orebody and the mining. Following Froyland et al. (2018), we assumed that the infrastructure is fixed throughout the mine life, the selling price of the product is known and the grade control is perfect. That is, once a block has been blasted, its contents are known perfectly.

As far as the orebody is concerned, the deposit was assumed to be part of a homogeneous rock mass, and secondly that the geostatistical parameters were perfectly known. The question

of parameter uncertainty, in particular the covariance or variogram model, has been addressed by several authors (Ortiz and Deutsch, 2002; Marchant and Lark, 2004; Emery and Ortiz, 2005; Pardo-Iguzquiza and Chica-Olmo, 2008; Olea and Pardo-Iguzquiza, 2011). As for the assumption that the orebody is part of a homogeneous mass, new Gaussian-based simulation techniques such as plurigaussian simulations (Armstrong et al., 2011) have been developed for simulating the layout of geological domains such as rock types or ore types. Although they were initially developed for the oil industry, they are now being applied in mining in a variety of geological settings, including uranium (Skvortsova et al., 2002), gold (Yunsel and Ersoy, 2011), lead-zinc (Yunsel and Ersoy, 2013), copper (Talebi et al., 2016; Maleki and Emery, 2015) and iron (Mery et al., 2017; Maleki et al., 2020). In our opinion, incorporating rock type uncertainty as well as grade uncertainty in stochastic mine production scheduling studies is one of the promising research avenues for the future.

6.1.2 Impact of the spatial covariance

In this work we used a well-structured spatial covariance, that is, one with a low nugget effect and a reasonably long range compared to the drill-hole spacing. While we ran tests for a range of drill-hole spacings, we did not test the effect of how well or how poorly the covariance was structured on the results. We suspect that they could have been quite different for poorly structured covariance models. Another direction for future research would therefore be to carry out tests for different covariance structures.

Acknowledgments

The authors would like to thank Eduardo Moreno (Universidad Adolfo Ibañez) for his help regarding the optimisation models. This research has been partially supported by the supercomputing infrastructure of the NLHPC (ECM-02) (University of Chile) and by the National Agency for Research and Development of Chile (ANID) with grants CONICYT/PIA/AFB180004 (X.E.), FONDECYT 1181513 (D.S) and FONDECYT 3180767 (G.L.).

References

M. Armstrong, A. Galli, H. Beucher, G. Loc'h, D. Renard, B. Doligez, R. Eschard, and F. Geffroy. *Plurigaussian simulations in geosciences*. Springer Science & Business Media, 2011.

M. W. A. Asad and R. Dimitrakopoulos. A heuristic approach to stochastic cutoff grade optimization for open pit mining complexes with multiple processing streams. *Resources Policy*, 38(4): 591–597, 2013.

J. Balzary and A. Mohais. Consideration for multi-objective metaheuristic optimisation of large iron ore and coal supply chains, from resource to market. In *Advances in Applied Strategic Mine Planning*, pages 297–316. Springer, 2018.

A. Ben-Tal, L. El Ghaoui, and A. Nemirovski. *Robust optimization*. Princeton University Press, 2009.

J. Benndorf. Making use of online production data: sequential updating of mineral resource models. *Mathematical Geosciences*, 47(5):547–563, 2015.

D. Bienstock and M. Zuckerberg. A new lp algorithm for precedence constrained production scheduling. *Optimization Online*, pages 1–33, 2009.

D. Bienstock and M. Zuckerberg. Solving lp relaxations of large-scale precedence constrained problems. In *International Conference on Integer Programming and Combinatorial Optimization*, pages 1–14. Springer, 2010.

A. Bley, A. M. Gleixner, T. Koch, and S. Vigerske. Comparing miqcp solvers to a specialised algorithm for mine production scheduling. In *Modeling, simulation and optimization of complex processes*, pages 25–39. Springer, 2012.

P. Bodon, C. Fricke, T. Sandeman, and C. Stanford. Combining optimisation and simulation to model a supply chain from pit to port. In *Advances in Applied Strategic Mine Planning*, pages 251–267. Springer, 2018.

N. Boland, I. Dumitrescu, and G. Froyland. A multistage stochastic programming approach to open pit mine production scheduling with uncertain geology. *Optimization Online*, 2008.

G. Canessa, E. Moreno, and B. K. Pagnoncelli. The risk-averse ultimate pit problem. *Optimization and Engineering*, URL: https://doi.org/10.1007/s11081-020-09545-4:1–24, 2020.

S. Chatterjee, M. R. Sethi, and M. W. A. Asad. Production phase and ultimate pit limit design under commodity price uncertainty. *European Journal of Operational Research*, 248(2):658–667, 2016.

C. Chevalier, X. Emery, and D. Ginsbourger. Fast update of conditional simulation ensembles. *Mathematical Geosciences*, 47(7):771–789, 2015.

J.-P. Chilès and P. Delfiner. *Geostatistics: modeling spatial uncertainty*. John Wiley & Sons, 2012.

G. Christakos. A bayesian/maximum-entropy view to the spatial estimation problem. *Mathematical Geology*, 22(7):763–777, 1990.

J. P. de Carvalho, R. Dimitrakopoulos, and I. Minniakhmetov. High-order block support spatial simulation method and its application at a gold deposit. *Mathematical Geosciences*, 51:793–810, 2019.

R. Dimitrakopoulos. *Advances in applied strategic mine planning*. Springer, 2018.

R. Dimitrakopoulos and A. Jewbali. Joint stochastic optimisation of short and long term mine production planning: method and application in a large operating gold mine. *Mining Technology*, 122(2):110–123, 2013.

R. Dimitrakopoulos and X. Luo. Generalized sequential gaussian simulation on group size nu and screen-effect approximations for large field simulations. *Mathematical Geology*, 36(5):567–591, 2004.

P. Dowd. Risk assessment in reserve estimation and open-pit planning. *Transactions of the Institution of Mining and Metallurgy (Section A: Mining Industry)*, 103, 1994.

P. Dowd and P. Dare-Bryan. Planning, designing and optimising production using geostatistical simulation. In *Advances in Applied Strategic Mine Planning*, pages 421–449. Springer, 2018.

X. Emery and C. Lantuéjoul. Tbsim: A computer program for conditional simulation of three-dimensional gaussian random fields via the turning bands method. *Computers & Geosciences*, 32(10):1615–1628, 2006.

X. Emery and J. M. Ortiz. Histogram and variogram inference in the multigaussian model. *Stochastic environmental research and risk assessment*, 19(1):48–58, 2005.

X. Emery, D. Arroyo, and E. Porcu. An improved spectral turning-bands algorithm for simulating stationary vector gaussian random fields. *Stochastic environmental research and risk assessment*, 30(7):1863–1873, 2016.

D. Espinoza, M. Goycoolea, E. Moreno, and A. Newman. Minelib: a library of open pit mining problems. *Annals of Operations Research*, 206(1):93–114, 2013.

P. I. Frazier. Bayesian optimization. In *Recent Advances in Optimization and Modeling of Contemporary Problems*, pages 255–278. INFORMS, 2018.

G. Froyland, M. Menabde, P. Stone, and D. Hodson. The value of additional drilling to open pit mining projects. In *Advances in Applied Strategic Mine Planning*, pages 119–138. Springer, 2018.

M. Gershon. Heuristic approaches for mine planning and production scheduling. *Geotechnical and Geological Engineering*, 5(1):1–13, 1987.

M. Godoy. A risk analysis based framework for strategic mine planning and design—method and application. In *Advances in Applied Strategic Mine Planning*, pages 75–90. Springer, 2018.

V. Goel and I. E. Grossmann. A class of stochastic programs with decision dependent uncertainty. *Mathematical programming*, 108(2-3):355–394, 2006.

J. J. Gómez-Hernández and A. G. Journel. Joint sequential simulation of multigaussian fields. In *Geostatistics Troia'92*, pages 85–94. Springer, 1993.

R. C. Goodfellow and R. Dimitrakopoulos. Global optimization of open pit mining complexes with uncertainty. *Applied Soft Computing*, 40:292–304, 2016.

P. Goovaerts. *Geostatistics for natural resources evaluation.* Oxford University Press on Demand, 1997.

S. Goria. *Evaluation d'un projet minier: approche bayésienne et options réelles.* PhD thesis, Paris, ENMP, 2004.

M. Goycoolea, D. Espinoza, E. Moreno, and O. Rivera. Comparing new and traditional methodologies for production scheduling in open pit mining. In *Proceedings of APCOM*, pages 352–359, 2015.

E. Henry, D. Marcotte, and M. Samis. Valuing a mine as a portfolio of european call options: The effect of geological uncertainty and implications for strategic planning. In *Geostatistics Banff 2004*, pages 501–510. Springer, 2005.

W. Hustrulid, M. Kuchta, and R. Martin. *Open Pit Mine Planning and Design.* CRC Press, 2013.

E. Jélvez, N. Morales, P. Nancel-Penard, J. Peypouquet, and P. Reyes. Aggregation heuristic for the open-pit block scheduling problem. *European Journal of Operational Research*, 249:1169–1177, 2016.

E. Jélvez, N. Morales, P. Nancel-Penard, and F. Cornillier. A new hybrid heuristic algorithm for the precedence constrained production scheduling problem: A mining application. *Omega*, 94: 102046, 2019.

A. Jewbali and R. Dimitrakopoulos. Implementation of conditional simulation by successive residuals. *Computers & geosciences*, 37(2):129–142, 2011.

A. Jewbali and R. Dimitrakopoulos. Stochastic mine planning—example and value from integrating long-and short-term mine planning through simulated grade control, sunrise dam, western australia. In *Advances in Applied Strategic Mine Planning*, pages 173–189. Springer, 2018.

T. B. Johnson. Optimum open pit mine production scheduling. Technical report, California Univ Berkeley Operations Research Center, 1968.

S. Khosrowshahi, W. Shaw, and G. Yeates. Quantification of risk using simulation of the chain of mining—case study at escondida copper, chile. In *Advances in Applied Strategic Mine Planning*, pages 57–74. Springer, 2018.

A. C. Kizilkale and R. Dimitrakopoulos. Optimizing mining rates under financial uncertainty in global mining complexes. *International Journal of Production Economics*, 158:359–365, 2014.

G. Lagos, D. Espinoza, E. Moreno, and J. Amaya. Robust planning for an open-pit mining problem under ore-grade uncertainty. *Electronic Notes in Discrete Mathematics*, 37:15–20, 2011.

T. Lagos, M. Armstrong, T. Homem-de Mello, G. Lagos, and D. Sauré. A framework for adaptive open-pit mining planning under geological uncertainty. *Optimization and Engineering*, URL: https://doi.org/10.1007/s11081-020-09557-0:1–36, 2020.

A. Lamghari. Mine planning and oil field development: a survey and research potentials. *Mathematical Geosciences*, 49(3):395–437, 2017.

C. Lantuéjoul. Ergodicity and integral range. *Journal of Microscopy*, 161(3):387–404, 1991.

C. Lantuéjoul. *Geostatistical simulation: models and algorithms*. Springer Science & Business Media, 2002.

H. Lerchs and I. F. Grossmann. Optimum design of open pit mines. *Transactions, The Canadian Institute of Mining and Metallurgy*, 68:17–24, 1965.

N. Mai, E. Topal, O. Erten, and B. Sommerville. A new risk-based optimisation method for the iron ore production scheduling using stochastic integer programming. *Resources Policy*, 62:571–579, 2019.

M. Maleki and X. Emery. Joint simulation of grade and rock type in a stratabound copper deposit. *Mathematical Geosciences*, 47(4):471–495, 2015.

M. Maleki, E. Jélvez, X. Emery, and N. Morales. Stochastic open-pit mine production scheduling: A case study of an iron deposit. *Minerals*, 10:585, 2020.

B. Marchant and R. Lark. Estimating variogram uncertainty. *Mathematical Geology*, 36(8):867–898, 2004.

G. Matheron. The intrinsic random functions and their applications. *Advances in applied probability*, 5(3):439–468, 1973.

J. McKinley, C. Deutscht, C. Neufeldt, M. Patton, M. Cooper, and M. Young. Use of geostatistical bayesian updating to integrate airborne radiometrics and soil geochemistry to improve mapping for mineral exploration. *Journal of the Southern African Institute of Mining and Metallurgy*, 114 (8):575–575, 2014.

C. Meagher, S. Abdel Sabour, and R. Dimitrakopoulos. Pushback design of open pit mines under geological and market uncertainties, the Australasian Institute of Mining and Metallurgy. *Spectrum Series*, 17:291–298, 2010.

M. Menabde, G. Froyland, P. Stone, and G. Yeates. Mining schedule optimisation for conditionally simulated orebodies. In *Advances in applied strategic mine planning*, pages 91–100. Springer, 2018.

N. Mery, X. Emery, A. Cáceres, D. Ribeiro, and E. Cunha. Geostatistical modeling of the geological uncertainty in an iron ore deposit. *Ore Geology Reviews*, 88:336–351, 2017.

M. Mokhtarian Asl and J. Sattarvand. Integration of commodity price uncertainty in long-term open pit mine production planning by using an imperialist competitive algorithm. *Journal of the Southern African Institute of Mining and Metallurgy*, 118(2):165–172, 2018.

E. Moreno, X. Emery, M. Goycoolea, N. Morales, and G. Nelis. A two-stage stochastic model for open pit mine planning under geological uncertainty. In *Proceedings of the 38th International Symposium on the Application of Computers and Operations Research in the Mineral Industry (APCOM)*, pages 13–27, 2017.

G. Muñoz, D. Espinoza, M. Goycoolea, E. Moreno, M. Queyranne, and O. R. Letelier. A study of the Bienstock–Zuckerberg algorithm: applications in mining and resource constrained project scheduling. *Computational Optimization and Applications*, 69(2):501–534, 2018.

H. Mustapha and R. Dimitrakopoulos. High-order stochastic simulation of complex spatially distributed natural phenomena. *Mathematical Geosciences*, 42(5):457–485, 2010.

A. M. Newman, E. Rubio, R. Caro, A. Weintraub, and K. Eurek. A review of operations research in mine planning. *Interfaces*, 40(3):222–245, 2010.

R. A. Olea and E. Pardo-Iguzquiza. Generalized bootstrap method for assessment of uncertainty in semivariogram inference. *Mathematical Geosciences*, 43(2):203–228, 2011.

D. S. Oliver and Y. Chen. Recent progress on reservoir history matching: a review. *Computational Geosciences*, 15(1):185–221, 2011.

D. S. Oliver, A. C. Reynolds, and N. Liu. *Inverse theory for petroleum reservoir characterization and history matching*. Cambridge University Press, 2008.

H. Omre. Bayesian kriging—merging observations and qualified guesses in kriging. *Mathematical Geology*, 19(1):25–39, 1987.

H. Omre and H. Tjelmeland. Petroleum geostatistics. In *Geostatistics Wollongong' 96*, pages 41–52. Kluwer, Dordrecht, 1997.

J. Ortiz and C. V. Deutsch. Calculation of uncertainty in the variogram. *Mathematical Geology*, 34(2):169–183, 2002.

M. Osanloo, J. Gholamnejad, and B. Karimi. Long-term open pit mine production planning: a review of models and algorithms. *International Journal of Mining, Reclamation and Environment*, 22(1):3–35, 2008.

A. Paithankar, S. Chatterjee, R. Goodfellow, and M. W. A. Asad. Simultaneous stochastic optimization of production sequence and dynamic cut-off grades in an open pit mining operation. *Resources Policy*, 66:101634, 2020.

E. Pardo-Iguzquiza and M. Chica-Olmo. Geostatistical simulation when the number of experimental data is small: an alternative paradigm. *Stochastic Environmental Research and Risk Assessment*, 22(3):325–337, 2008.

W. B. Powell and I. O. Ryzhov. *Optimal learning*, volume 841. John Wiley & Sons, 2012.

P. Ravenscroft. Risk analysis for mine scheduling by conditional simulation. *Transactions of the Institution of Mining and Metallurgy. Section A. Mining Industry*, 101, 1992.

M. Rezakhah, E. Moreno, and A. Newman. Practical performance of an open pit mine scheduling model considering blending and stockpiling. *Computers & Operations Research*, 115:104638, 2020.

A. Richmond. Direct net present value open pit optimisation with probabilistic models. In *Advances in applied strategic mine planning*, pages 217–228. Springer, 2018.

A. Rimélé, R. Dimitrakopoulos, and M. Gamache. A dynamic stochastic programming approach for open-pit mine planning with geological and commodity price uncertainty. *Resources Policy*, 65:101570, 2020.

M. A. Rimélé, R. Dimitrakopoulos, and M. Gamache. A stochastic optimization method with in-pit waste and tailings disposal for open pit life-of-mine production planning. *Resources Policy*, 57: 112–121, 2018.

A. Shapiro, D. Dentcheva, and A. Ruszczyński. *Lectures on stochastic programming: modeling and theory*. SIAM, 2009.

T. Skvortsova, H. Beucher, M. Armstrong, J. Forkes, A. Thwaites, and R. Turner. Simulating the geometry of a granite-hosted uranium orebody. In *Geostatistics Rio 2000*, pages 85–99. Springer, 2002.

A. Soares. Direct sequential simulation and cosimulation. *Mathematical Geology*, 33(8):911–926, 2001.

M. Spleit. Production schedule optimisation—meeting targets by hedging against geological risk while addressing environmental and equipment concerns. In *Advances in Applied Strategic Mine Planning*, pages 627–642. Springer, 2018.

P. Stone, G. Froyland, M. Menabde, B. Law, R. Pasyar, and P. Monkhouse. Blasor—blended iron ore mine planning optimisation at Yandi, Western Australia. In *Advances in Applied Strategic Mine Planning*, pages 39–46. Springer, 2018.

M. Tabesh and H. Askari-Nasab. Two-stage clustering algorithm for block aggregation in open pit mines. *Transactions of the Institution of Mining and Metallurgy - Section A: Mining Technology*, 120(3):158–169, 2011.

M. M. Tahernejad, R. Khalo Kakaei, and M. Ataei. Analyzing the effect of ore grade uncertainty in open pit mine planning; a case study of rezvan iron mine, iran. *International Journal of Mining and Geo-Engineering*, 52(1):53–60, 2018.

H. Talebi, E. Sabeti, M. Azadi, and X. Emery. Risk quantification with combined use of lithological and grade simulations: application to a porphyry copper deposit. *Ore Geology Reviews*, 75:42–51, 2016.

O. Tavchandjian, A. Proulx, and M. Anderson. Application of conditional simulations to capital decisions for Ni-sulfide and Ni-laterite deposits. In *Advances in Applied Strategic Mine Planning*, pages 319–333. Springer, 2018.

M. Vallejo and R. Dimitrakopoulos. Stochastic orebody modelling and stochastic long-term production scheduling at the kémag iron ore deposit, quebec, canada. *International Journal of Mining, Reclamation and Environment*, 33(7):462–479, 2019.

B. J. Willigers, S. Begg, and R. B. Bratvold. Combining geostatistics with bayesian updating to continually optimize drilling strategy in shale-gas plays. *SPE Reservoir Evaluation & Engineering*, 17(04):507–519, 2014.

A. M. Yaglom. Correlation theory of stationary and related random functions. *Volume I: Basic Results.*, 526, 1987.

T. Yunsel and A. Ersoy. Geological modeling of gold deposit based on grade domaining using plurigaussian simulation technique. *Natural Resources Research*, 20(4):231–249, 2011.

T. Yunsel and A. Ersoy. Geological modeling of rock type domains in the Balya (Turkey) lead-zinc deposit using plurigaussian simulation. *Central European Journal of Geosciences*, 5(1):78–89, 2013.

M. Zuckerberg, P. Stone, R. Pasyar, and E. Mader. Joint ore extraction and in-pit dumping optimization. *Orebody Modelling and Strategic Mine Planning AusIMM Spectrum Series*, 14(2): 137–140, 2007.